

Nuclear congression is driven by cytoplasmic microtubule plus end interactions in *S. cerevisiae*

Jeffrey N. Molk, E.D. Salmon, and Kerry Bloom

Department of Biology, University of North Carolina, Chapel Hill, NC 27599

Nuclear movement before karyogamy in eukaryotes is known as pronuclear migration or as nuclear congression in *Saccharomyces cerevisiae*. In this study, *S. cerevisiae* is used as a model system to study microtubule (MT)-dependent nuclear movements during mating. We find that nuclear congression occurs through the interaction of MT plus ends rather than sliding and extensive MT overlap. Furthermore, the orientation and attachment of MTs to the shmoo tip before cell wall breakdown is not required for nuclear congression. The MT plus end-binding proteins Kar3p, a class 14

COOH-terminal kinesin, and Bik1p, the CLIP-170 orthologue, localize to plus ends in the shmoo tip and initiate MT interactions and depolymerization after cell wall breakdown. These data support a model in which nuclear congression in budding yeast occurs by plus end MT capture and depolymerization, generating forces sufficient to move nuclei through the cytoplasm. This is the first evidence that MT plus end interactions from oppositely oriented organizing centers can provide the force for organelle transport *in vivo*.

Introduction

Little is known about how microtubules (MTs) overlap and function in living cells to promote haploid nuclear fusion, or karyogamy. The budding yeast *Saccharomyces cerevisiae* provides a genetic model system to study nuclear congression, the process in which haploid nuclei are moved toward each other (Rose, 1996). MTs are nucleated from the spindle pole body (SPB), and plus ends elongate into the cytoplasm (Fig. 1 A; Tirnauer et al., 1999; Lin et al., 2001; Maddox et al., 2003b). A MT plus end protein complex is formed to orient the nucleus and maintain the attachment of dynamic MT plus ends to the shmoo tip (Fig. 1 B; Miller and Rose, 1998; Maddox et al., 1999, 2003b). Attached MT plus ends switch between polymerization and depolymerization phases of dynamic instability, producing nuclear oscillations toward and away from the shmoo tip (Maddox et al., 1999). At the onset of cell fusion, MT plus ends from oppositely oriented mating cells are in proximity to one another (Fig. 1 C), ultimately facilitating MT–MT interactions. Nuclear oscillations cease after MT interactions are established, and MTs switch into a persistent depolymerization state during nuclear congression (Maddox et al., 1999). Once MTs have drawn both nuclei into proximity, karyogamy can begin.

A number of proteins bind MT plus ends and are required for karyogamy. The minus end-directed MT motor protein Kar3p concentrates at plus ends and is required to maintain depolymerizing MTs at the shmoo tip in addition to functioning in nuclear congression (Meluh and Rose, 1990; Maddox et al., 2003b). Nuclear translocation and orientation to the shmoo tip before cell fusion are actin dependent. Kar9p associates with the MT plus end-binding protein Bim1p, the budding yeast EB1 homologue, and the type V myosin Myo2p to link MTs to the polarized actin cytoskeleton (Hwang et al., 2003). Bik1p, the human CLIP-170 orthologue, binds MT plus ends to stabilize MT length and is critical for karyogamy (Berlin et al., 1990; Pellman et al., 1995; Lin et al., 2001). Both Bik1p and Kar9p are transported to the MT plus end by the kinesin-like protein Kip2p, but no role for Kip2p in karyogamy has been described (Miller et al., 1998; Maekawa et al., 2003; Carvalho et al., 2004).

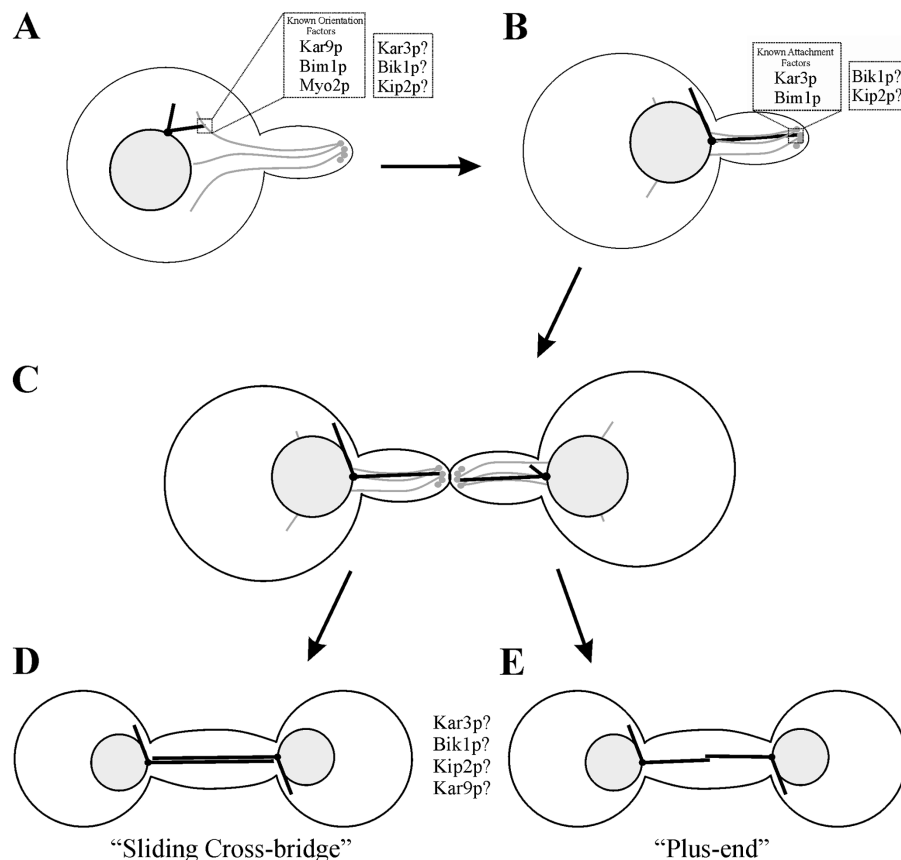
The main hypothesis for nuclear congression in living cells is a “sliding cross-bridge” mechanism in which, after cell fusion, MTs from opposite SPBs are thought to elongate past each other, producing a bundle of overlapping MTs of opposite orientation (Fig. 1 D; Rose, 1996). Kar3p, through its minus end-directed motility, is thought to cross-link the overlapping MTs and pull the SPBs together (Polaina and Conde, 1982; Meluh and Rose, 1990; Endow et al., 1994). In addition to sliding, the MTs are proposed to shorten as the SPBs come together. An unexplained puzzle in the sliding cross-bridge

Correspondence to Kerry Bloom: kerry_bloom@unc.edu

Abbreviations used in this paper: MT, microtubule; SPB, spindle pole body.

The online version of this article contains supplemental material.

Figure 1. Schematic of nuclear orientation, cytoplasmic MT attachment to the shmoo tip, and nuclear congression. Nucleus is gray; SPB is black circle; MTs are black bars; actin filaments are gray cables; actin patches are small gray circles. (A) Nuclear orientation to the shmoo tip. MTs are guided along filamentous actin toward the shmoo tip. Kar9p, Bik1p, and Myo2p are required for nuclear orientation, but the contributions of Kar3p, Bik1p, and Kip2p are unknown. (B) MT attachment to the shmoo tip. MTs are tethered to the mating projection by Kar3p during depolymerization and Bik1p during polymerization. Bik1p and Kip2p function in MT attachment is unknown. (C) Before cell-cell fusion, MTs are maintained at the shmoo tip. (D) Sliding cross-bridge model for nuclear congression. Oppositely oriented MTs overlap and are cross-linked along their lengths, whereas depolymerization is induced at the spindle poles (Rose, 1996). (E) Plus end model for nuclear congression. MT plus ends cross-link and induce depolymerization to draw opposing nuclei together. In either the sliding cross-bridge or plus end models, the localization and/or function of Kar3p, Bik1p, Kip2p, and Kar9p during live cell nuclear congression is not known.



model is what coordinates MT depolymerization with sliding, because MT shortening occurs as the two SPBs and attached nuclei come together. The sliding cross-bridge model proposes that Kar3p depolymerizes MTs from the minus end at the spindle poles, although this was based on early *in vitro* studies (Endow et al., 1994; Rose, 1996). Thus far, fluorescent marks on MTs indicate that both polymerization and depolymerization occur solely at the plus ends (Maddox et al., 1999, 2000; Tanaka et al., 2005). Additionally, a recent *in vitro* study demonstrated that Kar3p is a plus end MT depolymerase (Sproul et al., 2005). These data suggest that proteins at the plus ends regulate polymerization and depolymerization and could both tether dynamic plus ends to the shmoo tip and perform nuclear congression. In the sliding cross-bridge model, plus ends should be found near the SPBs during nuclear congression.

An alternative model for nuclear congression arises from the proximity of plus end-binding proteins on MTs at the shmoo tip before cell fusion (Fig. 1 E). In the plus end model, linkage of MTs from opposite SPBs occurs when plus end complexes interact. MT depolymerization would provide the force to pull the nuclei together. This model predicts that plus end complexes remain concentrated at the site where MTs from oppositely oriented SPBs contacted each other after cell fusion.

To determine by what mechanism nuclear congression occurs, MTs and plus end-binding proteins were analyzed in living *S. cerevisiae* cells. Before nuclear congression, Kar3p, Bik1p, and Kip2p were required for the anchorage of MT plus ends to the shmoo tip. After cell fusion, MT plus ends inter-

acted stochastically to drive nuclear congression. Bik1p and Kar3p localized to oppositely oriented MT plus ends that interacted near the site of cell fusion in wild-type cells. As nuclear congression occurred, the positions of the plus ends were unchanged as SPBs moved inward. By analyzing karyogamy mutants, our data suggested that Kar3p was required to initiate MT plus end interactions, whereas Bik1p promoted persistent MT interactions during nuclear congression. Kar9p contributed to the fidelity of nuclear congression by guiding plus ends toward each other. These data support a model in which oppositely oriented MTs interact and depolymerize at their plus ends to draw opposing nuclei together in *S. cerevisiae*.

Results

Kar3p and Bik1p are required for coupling dynamic MTs to the shmoo tip

Kar9p, Bik1p, and Kar3p are required for karyogamy after cell fusion (Berlin et al., 1990; Meluh and Rose, 1990; Kurihara et al., 1994). *kar3Δ* mutants have the most severe nuclear congression defect, followed by *bik1Δ* and *kar9Δ* cells (Fig. 2). To test whether defective nuclear congression was preceded by a defect in nuclear orientation to the shmoo tip, GFP-Tub1p-marked SPBs and MTs were examined. In wild-type cells, nuclear orientation occurred when the SPB was inside or near the base of the shmoo tip (Fig. 3 A and Table S1, available at <http://www.jcb.org/cgi/content/full/jcb.200510032/DC1>). As expected, *kar9Δ* cells had a nuclear orientation defect (Miller and Rose, 1998), and the SPB

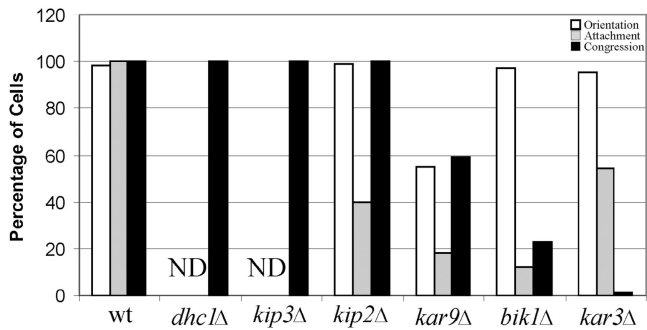


Figure 2. Percentage of successful nuclear orientation, cytoplasmic MT attachment to the shmoo tip, and nuclear congression in karyogamy mutants. Nuclear orientation, white bars; cytoplasmic MT attachment, gray bars; nuclear congression, black bars. Nuclear orientation was scored as successful if the SPB, marked by GFP-Tub1p, was positioned in or near the base of the shmoo tip. Cytoplasmic MT attachment to the shmoo tip was determined using the degree of persistence or the amount of time MTs remained attached to the shmoo tip in consecutive frames during time-lapse imaging. Nuclear congression was scored as wild-type if both SPBs were fused into a single GFP-Tub1p focus or two closely associated foci ($\sim 0.5 \mu\text{m}$). Nuclear orientation and cytoplasmic MT attachment in *dhc1Δ* and *kip3Δ* was not scored (ND; see Maddox et al., 2003b for relative measurements).

was positioned in the cell body distal to the shmoo tip (Table S1). However, nuclear orientation to the shmoo tip occurred in the absence of Bik1p and Kar3p (Fig. 3 and Table S1). Additionally,

Kip2p was not required for nuclear orientation (Fig. 3 and Table S1; Miller et al., 1998). Therefore, the nuclear congression defects characterized for *kar3Δ* and *bik1Δ* mutants do not result from a general defect in nuclear orientation.

After nuclear orientation in wild-type cells, MTs remain attached to the shmoo tip (Maddox et al., 1999). The persistence of MT plus end attachment at the shmoo tip was measured by the percentage of time that continuous GFP-Tub1p fluorescence extended from the SPB to the shmoo tip in time-lapse records. In wild-type cells, the degree of persistence was 100%, indicating that the attachment of one or more MTs was continuously maintained at the shmoo tip (Fig. 3 A, Table S1, and Video 1). The attachment was not persistent in *kar3Δ* cells when MTs switched to depolymerization (Fig. 3 B and Table S1; Miller and Rose, 1998; Maddox et al., 2003b). Similarly, the degree of persistence was reduced in *bik1Δ* and *kip2Δ* mutants (Fig. 3, C and D; Video 1, and Table S1). In these cells, detachment occurred when MTs switched to depolymerization. Therefore, like Kar3p, Bik1p is required to maintain depolymerizing MT plus ends at the shmoo tip.

During mitosis, Bik1p localizes to both growing and shortening MT plus ends in the cytoplasm (Carvalho et al., 2004). In pheromone-treated cells, Bik1p-3xGFP localized predominantly to MT plus ends in the shmoo tip and marked growing and shortening MT plus ends (Fig. 4). The incorporation

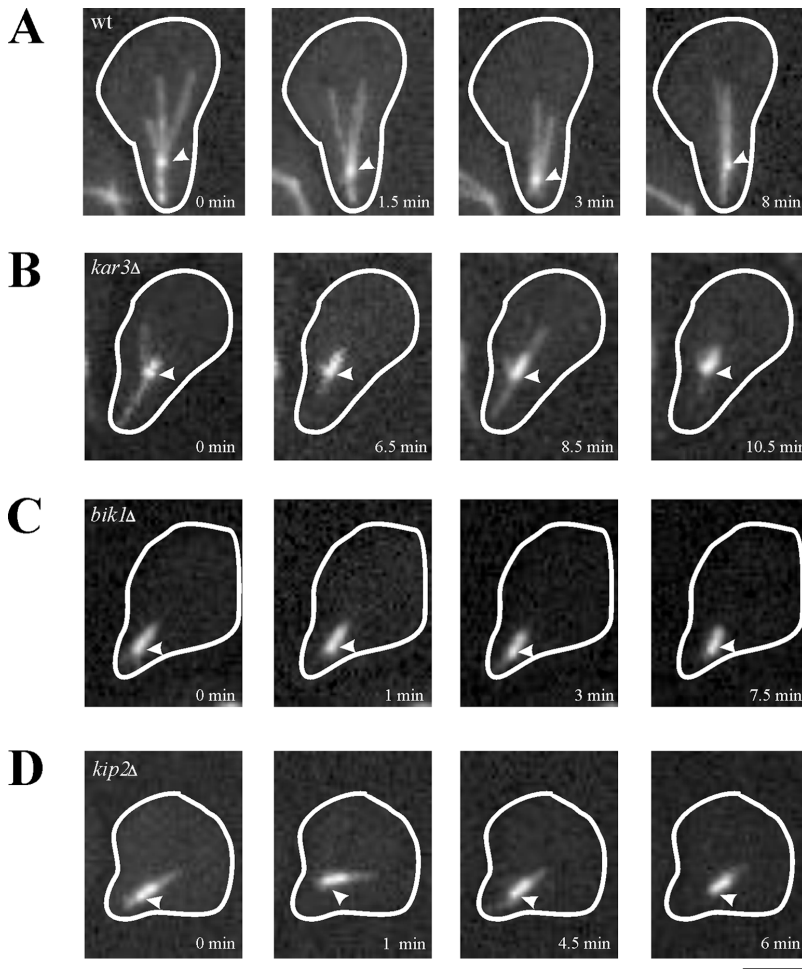
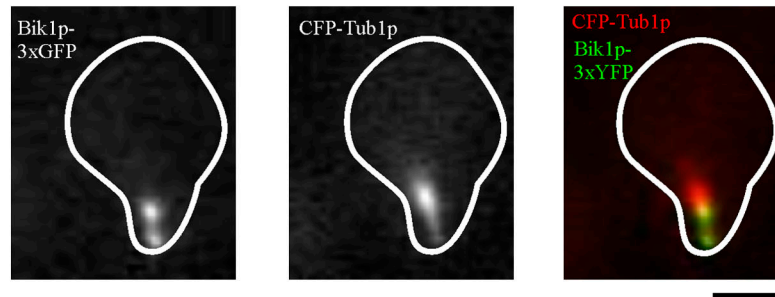
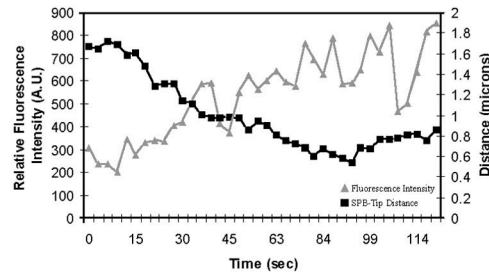
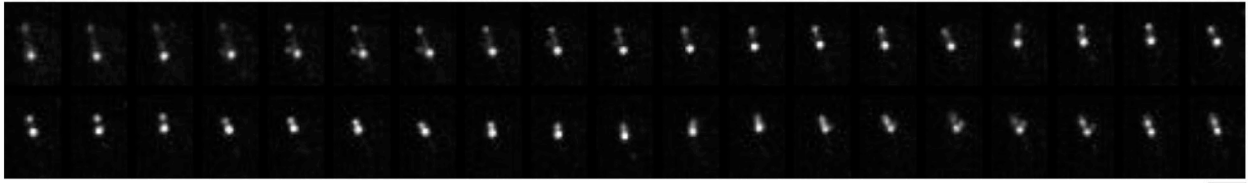


Figure 3. Cytoplasmic MT attachment to the mating projection is not persistent in *kar3Δ*, *bik1Δ*, or *kip2Δ* cells. Arrowheads denote the positions of SPBs, marked by GFP-Tub1p fluorescence, relative to the shmoo tip. (A) Wild-type (wt) cells displayed persistent attachment of cytoplasmic MTs to the shmoo tip (0 min), whereas the SPB oscillates along the polarity axis of the cell (1.5, 3, and 8 min). (B) *kar3Δ* cells with cytoplasmic MT attachment to the shmoo tip (0 min) detached upon depolymerization (6.5 min) and regained attachments upon polymerization toward the mating projection (8.5 min). New attachments were lost during a second depolymerization event (10.5 min). (C) *bik1Δ* cells have short cytoplasmic MTs that were attached to the mating projection (0 min) and detached as depolymerization occurred (1 min). New attachments were gained and lost during the time lapse (3 and 7.5 min). (D) *kip2Δ* cells with short cytoplasmic MT attachments to the shmoo tip (0 min) lost the attachment (1 min), regained it, and then lost the attachment (4.5 and 6 min). The GFP-Tub1p fluorescence in *kip2Δ* cells distal from the shmoo tip marked the SPB (wild-type SPB $1.87 \mu\text{m}$ from the shmoo tip; *kip2Δ* SPB is $1.64 \mu\text{m}$ from the shmoo tip; $P > 0.09$; $n = 20$ cells each). Bar, $2 \mu\text{m}$.

A



B



C

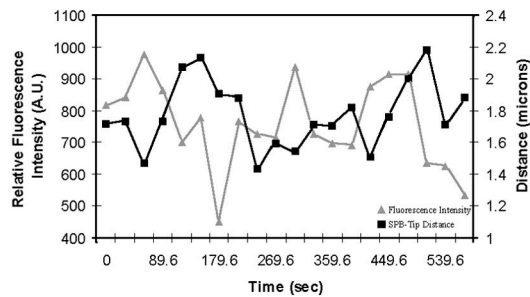
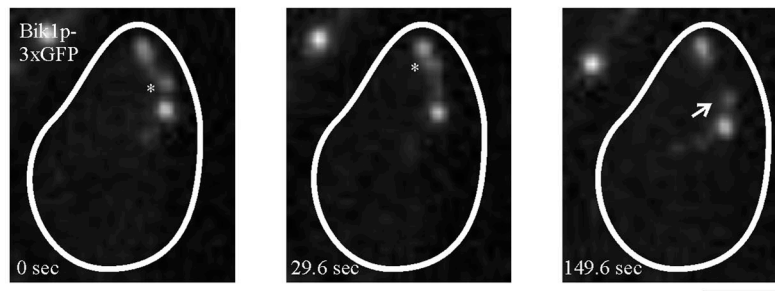
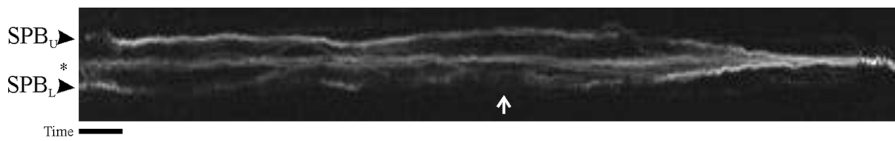
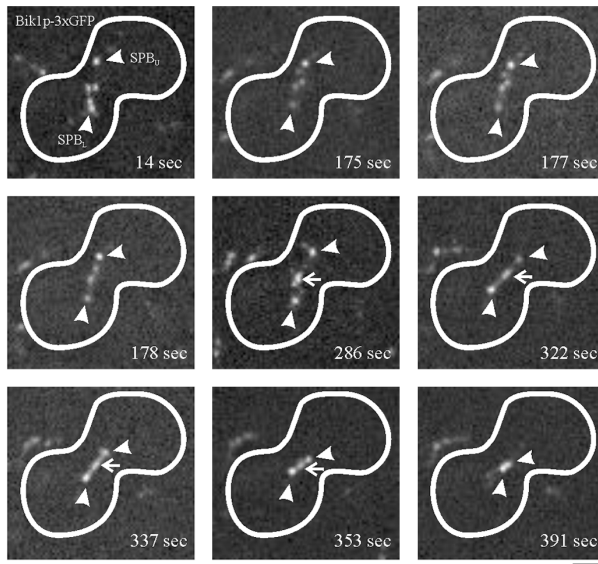


Figure 4. **Bik1p-3xGFP localized to the shmoo tip and SPB in cells challenged with mating pheromone.** (A) Bik1p-3xGFP colocalization with CFP-Tub1p by wide-field microscopy. Left panel is Bik1p-3xGFP; middle panel is CFP-Tub1p fluorescence; right panel is an overlay of Bik1p-3xGFP in green and CFP-Tub1p in red. Bik1p localized to both the shmoo tip and SPB. (B) Bik1p-3xGFP localization in pheromone-treated cells. Top panel is a montage from time-lapse imaging of Bik1p-3xGFP. Single planes were acquired approximately every 3 s. Note the enrichment of Bik1p-3xGFP at the shmoo tip (facing up) during depolymerization. (B and C) Bottom panel is a plot of Bik1p-3xGFP fluorescence intensity (gray triangles) and distance from the SPB (black squares) to the shmoo tip over time. As the SPB moved toward the shmoo tip, Bik1p-3xGFP fluorescence on MT plus ends at the mating projection increased. (C) Bik1p-3xGFP localization in pheromone-treated cells. Top panel is time-lapse imaging of Bik1p-3xGFP localization in the mating projection. Five-plane Z-series were acquired every 30 s, and maximum projection images are presented. Asterisks denote Bik1p-3xGFP-marked MT plus ends that incorporate into the shmoo tip; arrow signifies Bik1p-3xGFP localization to a newly nucleated MT plus end. Note Bik1p-3xGFP localization on nonshmoo tip MTs facing the cell body (149.6 s). Bik1p-3xGFP increased in fluorescence intensity as the SPB moved toward the shmoo tip and decreased in fluorescence intensity as the SPB-to-shmoo tip distance increased. Bars, 2 μ m.

A



B

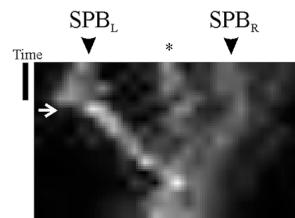
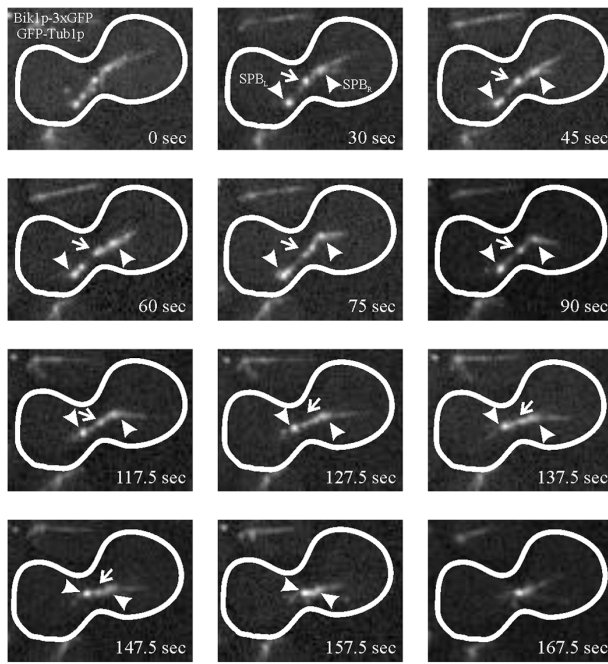


Figure 5. Wild-type nuclear congression occurs by MT plus end cross-linking and depolymerization. (A) Top panel (14 s) shows cells of opposite mating types expressing Bik1p-3xGFP. Arrowheads denote SPBs (upper SPB, SPB_U; lower SPB, SPB_L). (175–178 s) Bik1p-3xGFP plus ends cross-link during nuclear congression. New MT plus ends could incorporate into the plus ends that cross-linked opposite MTs during nuclear congression (Video 5, available at <http://www.jcb.org/cgi/content/full/jcb.200510032/DC1>). (286 s) Initial interactions between plus ends labeled with Bik1p-3xGFP, noted by arrow. (322–391 s) Nuclear congression occurred, and SPBs moved in toward the site of initial plus end interactions. Arrows point to the site where MT plus ends that were nucleated from opposite SPBs interact. Bottom panel shows kymograph of nuclear congression. Time bar, ~20 s (calibrated for 1-s intervals taken during the bulk of imaging). Asterisk denotes plus end Bik1p-3xGFP signal; arrow marks approximate time of plus end fusion. SPBs move inward to the region where plus ends interacted during nuclear congression. (B) Top panel (0 s) shows a cell expressing Bik1p-3xGFP (left) mated to a cell expressing GFP-Tub1p (right). (30 s) Oppositely oriented MTs associated in a single Bik1p-3xGFP focus (arrows) in between the two SPBs (arrowheads; left SPB, SPB_L; right SPB, SPB_R). (45–75 s) MTs remained associated with the Bik1p-3xGFP focus as SPB position changed. (90–147.5 s) SPBs began to move toward each other as nuclear congression occurred. Note the stable position of the Bik1p-3xGFP focus as the SPBs moved inward. (157.5 and 167.5 s) The SPBs became one focus before nuclear fusion. Bottom panel shows kymograph of nuclear congression. Time bar, ~90 s. Asterisk denotes Bik1p-3xGFP focus; arrow marks approximate time of plus end fusion. The SPBs move inward toward the Bik1p-3xGFP focus that maintained its position during nuclear congression. Bars, 2 μm.

of new plus ends into the shmoo tip bundle could increase the fluorescence intensity over time (Fig. 4, B and C; and Video 2). Bik1p-3xGFP fluorescence intensity at the shmoo tip accumulated when the distance from the SPB to the shmoo tip decreased

(Fig. 4 B). Conversely, the fluorescence intensity diminished when the SPB–shmoo tip distance increased (Fig. 4 C). This suggests that Bik1p may anchor shortening MT plus ends to the shmoo tip similarly to Kar3p (Maddox et al., 2003b).

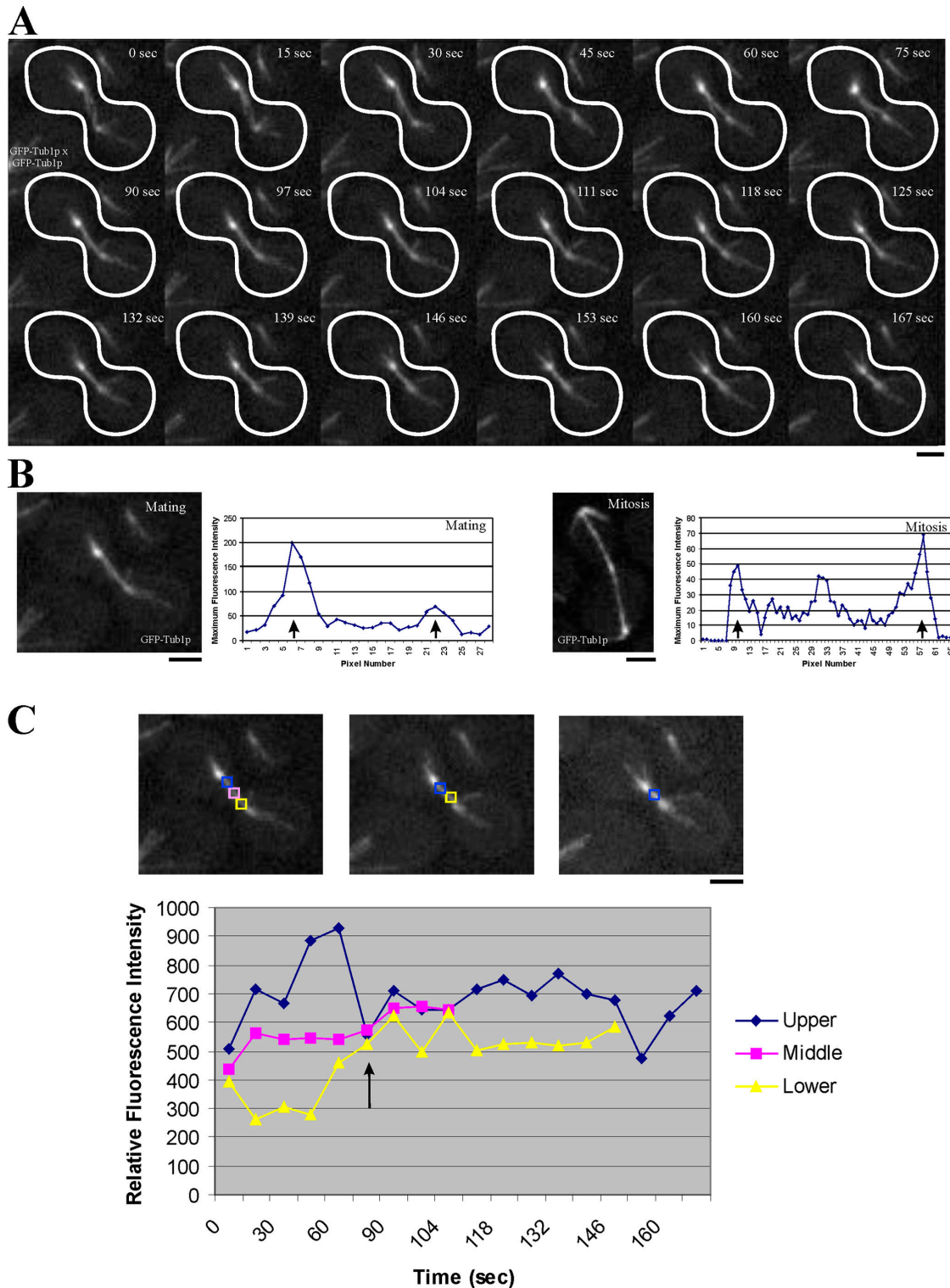


Figure 6. GFP-Tub1p fluorescence intensity between SPBs does not increase during nuclear congression. (A) Montage of wild-type cells expressing GFP-Tub1p during nuclear congression. Nuclear congression begins at ~ 97 s, and both SPBs move in toward the region of initial plus end MT interactions. (B) Comparisons of MT overlap fluorescence during mating (left) and mitosis (right). Images are projections of five-plane Z-series. Arrows mark positions of the SPBs. From the time of initial MT interactions through the time-lapse images, mating cells show two major peaks of fluorescence at the SPBs. In contrast, mitotic cells have a third peak corresponding to overlapping MTs in the midzone ($n = 5$ cells each). (C) Top panels are descriptions of fluorescence intensity analysis for GFP-Tub1p cells during nuclear congression. Three nonoverlapping 5×5 pixel boxes (left) were placed between, but not including, the two SPBs to record the integrated fluorescence intensity in the region before and after nuclear congression. Background was subtracted by moving the boxes to nearby regions in the cell without GFP-Tub1p fluorescence. As nuclear congression began, the area became best fit by two boxes (middle) and then a single box (right). Bottom panel shows fluorescence intensity measurements of GFP-Tub1p during nuclear congression. Arrow denotes the beginning of nuclear congression. The integrated fluorescence intensity from the top (blue), middle (pink), and bottom box (yellow) was recorded and plotted versus time. If sliding was the mechanism of nuclear congression, the fluorescence intensity of the middle box and two outer boxes should equal the sum of the

Nuclear congression occurs when MT plus ends interact

A critical difference between the sliding cross-bridge and plus end models is the position of MT plus ends during nuclear congression. To determine the distribution of MT plus ends, we examined Bik1p-3xGFP or Kar3p-GFP during nuclear congression. In 82% of cells, these proteins localized as a focus in between both SPBs before and during nuclear congression ($n = 23/28$ cells). Using Bik1p-3xGFP to label plus ends, we acquired single plane images at 1-s intervals. Before nuclear congression, MT plus ends concentrated at the shmoo tips, and newly nucleated MTs could elongate and become incorporated into the shmoo tip bundle (Video 3). Once shortening was activated, SPBs moved in toward the position of the initial plus end interactions (Fig. 5 A and Video 3). The two sets of plus ends joined into a single Bik1p-3xGFP focus that persisted after nuclear congression began (Fig. 5 A, 286–391 s; arrows). SPBs moved in toward the Bik1p-3xGFP focus at $1.08 \pm 0.72 \mu\text{m}/\text{min}$ ($n = 6$ cells), and nuclear congression could be completed in as little as 2 min. During nuclear congression, newly nucleated MTs could incorporate into or be released from the Bik1p-3xGFP focus but were not seen to cross over toward the other SPB (Video 3). Kymographs demonstrated that the two SPBs moved in toward the site of plus end interactions during nuclear congression ($n = 5$ cells; Fig. 5 A, bottom).

To ensure that Bik1p-3xGFP was labeling MT ends during nuclear congression, we mated GFP-Tub1p-expressing cells with Bik1p-3xGFP cells (Fig. 5 B) and imaged them in three dimensions over time. A single Bik1p-3xGFP focus was observed at the site of MT tip interaction (Fig. 5 B, 30–90 s; arrows). Occasional spreading of the Bik1p-3xGFP signal from a distinct focus to a more diffuse localization along the MT was visible at later time points (Fig. 5 B, 117.5–167.5 s). The position of the Bik1p-3xGFP focus did not significantly change as SPBs moved inward (Fig. 5 B, bottom). Kar3p-GFP also localized as a single focus between the two SPBs in mating cells (Fig. S1, available at <http://www.jcb.org/cgi/content/full/jcb.200510032/DC1>). Thus, during nuclear congression, MT plus ends from opposing SPBs interact, and depolymerization likely drives the SPBs together for nuclear fusion.

If the plus end depolymerization model is the predominant mechanism for nuclear congression, the zone of MT overlap should be small or undetectable (Fig. 6 A and Video 4). Line scans of GFP-Tub1p during nuclear congression showed two peaks of fluorescence that corresponded to the SPBs with no detectable overlap zone (Fig. 6 B, left panels). Additionally, measurements of the fluorescence intensity before and during nuclear congression were analyzed (Fig. 6 C). If MTs slide past each other before nuclear congression, the fluorescence should be additive. However, after MT plus end

interactions occurred (Fig. 6 C, graph; arrow), the GFP-Tub1p fluorescence did not increase as SPBs moved inward (Fig. 6 C, graph).

As a positive control, MT overlap in the central spindle during anaphase of mitosis was analyzed. Line scans of the central spindle displayed three peaks: two representing SPBs (Fig. 6 B, graphs; arrows) and one at the midzone (Fig. 6 B, right panels). This demonstrates that overlap between one to two MTs (O'Toole et al., 1999) can be detected. The lack of MT overlap and the localization of Bik1p and Kar3p to a single focus indicate that plus end linkages are the predominant anchorage mechanism for nuclear congression.

Nuclear congression does not require prior nuclear orientation

The karyogamy defect in the nuclear orientation mutant *kar9Δ* is not as severe as other karyogamy mutants (Fig. 2). One possible explanation is that in the absence of nuclear orientation, oppositely oriented MT plus ends use a stochastic search-and-capture mechanism to interact and promote nuclear congression. To test this hypothesis, *kar9Δ* cells with separated SPBs were examined after cell fusion (Fig. 7 and Video 5). MTs were seen to grow and shrink in the cytoplasm (Fig. 7, 3–7 min), and lateral MT interactions, which were visible in the same focal plane, did not move SPBs together (Fig. 7, 7.5–13 min). In contrast, nuclear congression did occur when MT tips contacted each other (Fig. 7, 17–18.5 min; $n = 5/6$ cells). Therefore, MT plus end interactions, but not orientation to the shmoo tip, are required for nuclear congression in *kar9Δ* cells.

Bik1p is required for persistent MT interactions during nuclear congression

Bik1p is required for the formation or stability of MTs in mating cells (Berlin et al., 1990) and is delivered to MT plus ends by Kip2p. Bik1p-3xGFP localized predominantly to the SPB in *kip2Δ* cells with diminished localization at presumptive MT plus ends ($n = 117/118$ cells; Fig. 8 A and Video 6). The low level of Bik1p-3xGFP at plus ends in *kip2Δ* cells is not sufficient to promote persistent attachment of MTs to the shmoo tip (Table S1). However, despite the shorter length of MTs, there is no mating defect in *kip2Δ* cells (Table S2; Miller et al., 1998). Thus, MT length is not the critical parameter for nuclear congression, and reduced levels of Bik1p on the plus ends appear sufficient to support karyogamy but not persistent attachment to the shmoo tip.

To ensure that the delivery of Bik1p to the plus end was specific to Kip2p, *kar3Δ* cells were also examined. Bik1p-3xGFP labeled both polymerizing and depolymerizing MT plus ends in the shmoo tip as well as the SPB of *kar3Δ* cells (Fig. 8 A and Video 7), suggesting that the shmoo tip attachment

fluorescence intensity before MT cross-linking. The fluorescence before MT interactions occurred could fluctuate as newly nucleated MTs were incorporated into the MT bundle (0–90 s, yellow line). However, the fluorescence did not double in this region before or during nuclear congression after MT–MT interactions were established, suggesting that the sliding of MTs does not occur during nuclear congression. This result was seen in all cells imaged and analyzed ($n = 5$). Bars, 2 μm .



Figure 7. **Nuclear congression occurred in the absence of Kar9p.** (0–8 min) SPB motility as a result of MT–cortical interactions changed spindle pole position without resulting in nuclear congression. (8.5–12.5 min) An apparent lateral MT interaction did not result in nuclear congression. (13.5 and 17 min) SPBs were positioned to face each other, and MTs grew toward each other. (17.5 min) MTs interacted at the plus end to begin nuclear congression. (18 and 18.5 min) Nuclear congression was completed as both SPBs were drawn toward each other. Bar, 2 μ m.

and karyogamy defects observed in *kar3Δ* cells do not result from Bik1p mislocalization.

If MT length is not a critical factor governing nuclear congression, Bik1p could be required to promote persistent interactions between MTs. Alternatively, Bik1p could be a factor that directly links plus ends to promote nuclear congression. In *bik1Δ* mutants expressing GFP-Tub1p, MTs were short and rapidly depolymerized back to the SPBs, limiting the ability of oppositely oriented MTs to interact (Fig. S2, available at <http://www.jcb.org/cgi/content/full/jcb.200510032/DC1>). This phenotype resulted in a large fraction of cells (10/13 cells) that did not perform nuclear congression. In those cells where nuclear congression did occur, MTs appeared to interact without rapidly shortening back to the SPBs (Fig. 8 B and Video 8). Despite the instability of MT interactions in *bik1Δ* cells, the MTs could remain associated long enough to draw the opposing SPBs together (Fig. 8 B, 11 and 14 min). These data sug-

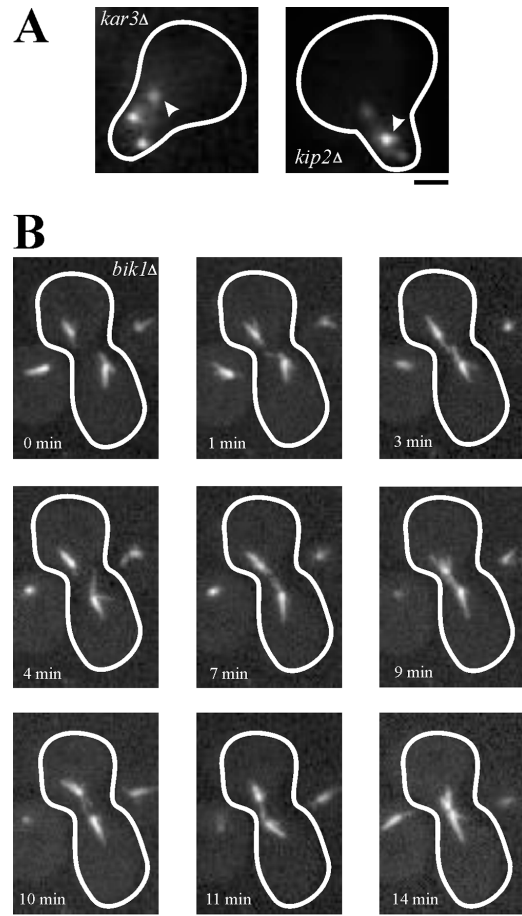


Figure 8. **Bik1p is required for persistent MT interactions during nuclear congression.** (A) Bik1p-3xGFP localization in *kar3Δ* and *kip2Δ* cells. Left panel shows that in the absence of Kar3p, Bik1p-3xGFP localized to both growing and shortening MTs in the shmoo tip, a result of the *kar3Δ* attachment defect. Right panel shows that Bik1p-3xGFP localization on shmoo tip and nonshmoo tip MTs was reduced but still visible in *kip2Δ* cells. Arrowheads denote the positions of SPBs. (B) Nuclear congression in *bik1Δ* cells expressing GFP-Tub1p. Separated SPBs close to the center of the cell body (0 min) nucleated short MTs (1 min) that were in proximity to each other (3–7 min). The increased fluorescence facing away from the site of cell fusion likely represents nuclear tubulin fluorescence. MTs from opposing spindle poles appeared to cross-link (9 min), although this linkage broke (10 min) and reformed (11 min) to ultimately allow nuclear congression (14 min). Bars, 2 μ m.

gest that Bik1p promotes persistent MT–MT interactions or contributes to plus end linkage during nuclear congression.

Kar3p is required for MT plus end interactions during nuclear congression

Kar3p may be the key component in MT plus end interactions during nuclear congression. In bilateral crosses of *kar3Δ* mutants, the MTs were longer than in wild-type cells, and MTs did not interact to perform nuclear congression (Fig. 9 A and Video 9). Unlike *kar9Δ* cells, MT plus ends passed each other without interacting in *kar3Δ* mutants (Fig. 9 A, 0–29 min). No MT plus end interactions were observed when *kar3Δ* strains expressing Bik1p-3xGFP crossed to GFP-Tub1p were imaged (Fig. S3), and nuclear congression was rarely seen in *kar3Δ* bilateral crosses (18/19 cells with no congression). Thus, Kar3p

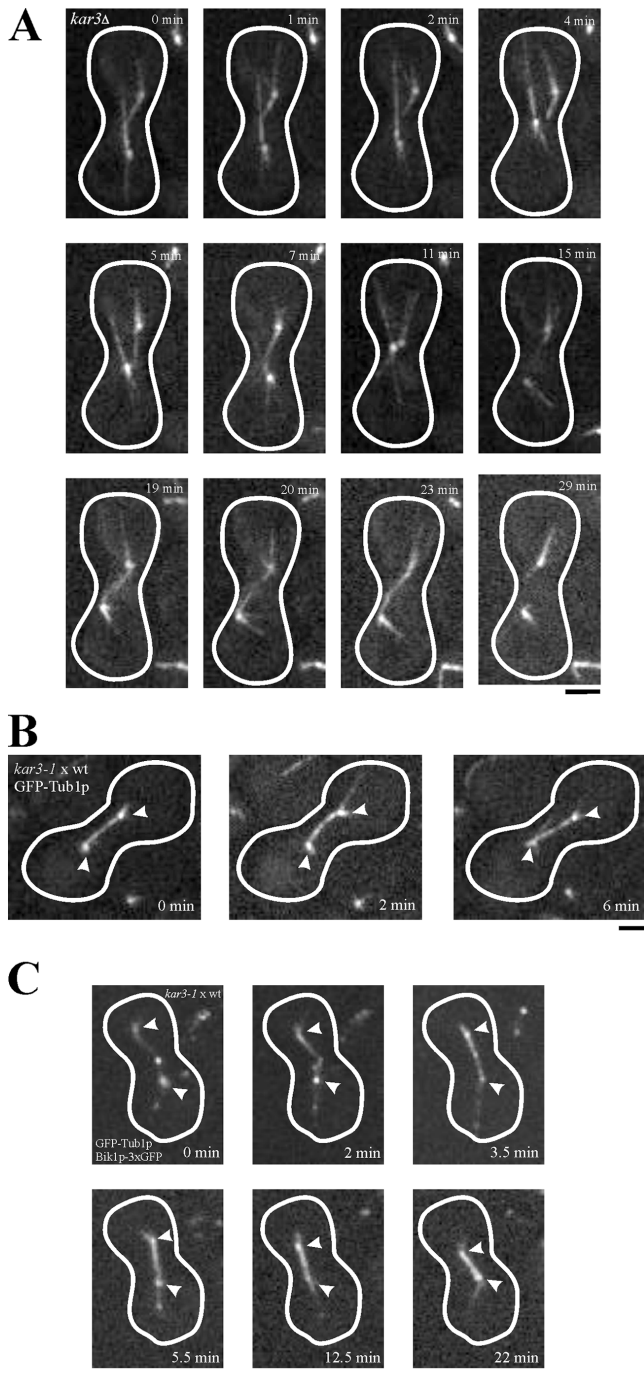


Figure 9. Kar3p is required to cross-link and shorten MTs during nuclear congression. (A) MT behavior in bilateral *kar3Δ* crosses. (0–7 min) Long cytoplasmic MTs interacted with opposing MTs without resulting in nuclear congression. (11 and 15 min) SPBs were drawn together, but nuclear congression did not occur. (19–29 min) MTs appeared to interact at the plus end, but these interactions did not change SPB position or result in nuclear congression. (B) *kar3-1* mutants that were mated to wild-type cells resulted in cross-linked MTs that did not shorten. Arrowheads denote SPBs. (0–6 min) Two SPBs were separated by a GFP-Tub1p bridge of cross-linked MTs. (C) *kar3-1* cells expressing GFP-Tub1p mated to wild-type cells expressing Bik1p-3xGFP. Arrowheads denote SPBs. (0 min) Bik1p-3xGFP localizes to MT plus ends in the shmoo tip. (2 min) Initial MT–MT interactions occurred. (3.5 min) MTs are cross-linked without a strong Bik1p-3xGFP focus in between SPBs. (5.5–22 min) No Bik1p-3xGFP focus is present as MTs remain associated. Some movement of SPBs toward each other occurs over time. Bars, 2 μm.

is required to promote the persistent interaction of oppositely oriented MT plus ends during nuclear congression before the switch to coordinated MT depolymerization occurs.

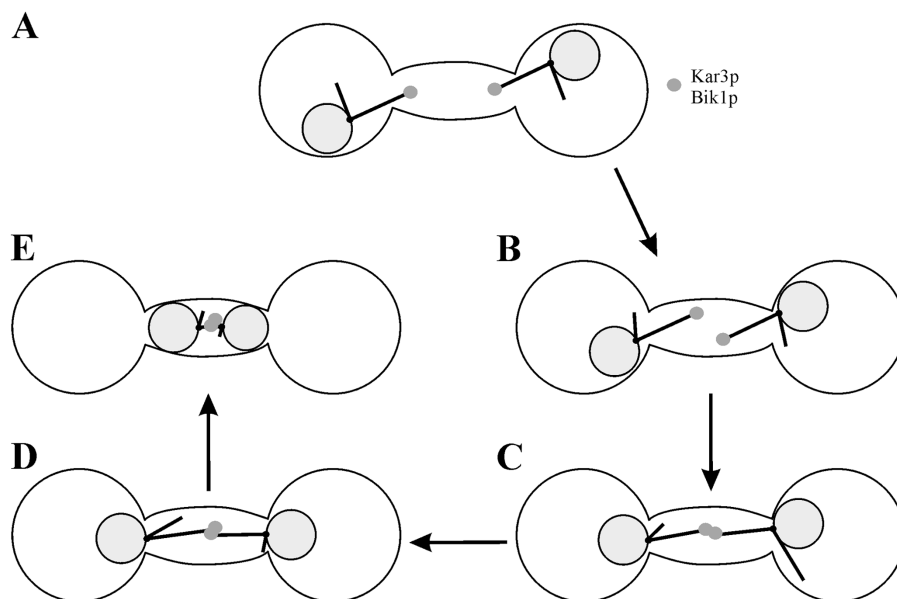
kar3-1 cells contain a constitutive point mutation in *KAR3* that results in rigor binding of the motor head to the MT and generates a semidominant mating defect (Polaina and Conde, 1982; Meluh and Rose, 1990). In the sliding cross-bridge model, Kar3p should act along the length of MTs to promote MT interactions. *kar3-1p* localizes along the length of the MT instead of concentrating at the plus end (Meluh and Rose, 1990; Maddox et al., 2003b). If plus end interactions drive nuclear congression, failing to concentrate Kar3p at the plus ends may prevent nuclear congression from occurring. When *kar3-1* was the only source of Kar3p in the cell, MTs did not interact, and nuclear congression did not occur (8/8 cells with no congression; see Fig. 9 A for a representative example). Therefore, rigor-bound Kar3p is not sufficient for nuclear congression.

In contrast, mating *kar3-1* cells to wild-type cells resulted in a single bridge of GFP-Tub1p fluorescence between the two SPBs in ~50% of cells (Fig. 9 B). The rigor-bound *kar3-1* prevented complete MT depolymerization in these cells but did not prevent the persistence of MT–MT interactions (10/11 cells with no congression). A single focus of plus ends, visualized by Bik1p-3xGFP, did not form between the two SPBs ($n = 6$ cells; Fig. 9 C and Video 10). Bik1p-3xGFP redistributed from a single focus in the wild-type cell before cell fusion to a diffuse localization along the MTs as cross-linking occurred after cell fusion (Fig. 9 C, 3.5–5.5 min). This indicates that when *kar3-1p* bound to the MT lattice encounters Kar3p, interactions are no longer restricted to the plus end. Thus, Kar3p localization at the plus end initiates MT–MT interactions during nuclear congression.

Discussion

The sliding cross-bridge model for nuclear congression arose from the genetic and biochemical analysis of karyogamy (Rose, 1996). Considering recent data that demonstrates MTs assemble and disassemble from the plus end and that proteins localized to the plus ends play a critical role in nuclear migration during mitosis (Maddox et al., 2000; Lee et al., 2003; Sheeman et al., 2003), an examination of nuclear congression was warranted. Does nuclear congression occur by the sliding of oppositely oriented MTs or by force generation coupled to plus end depolymerization? Our data indicate that depolymerization of the MT plus end brings two haploid nuclei together to form a diploid nucleus in budding yeast. Rather than cross-linking along the length of oppositely oriented MTs, a complex comprised minimally of Bik1p and Kar3p localizes to MT plus ends originating from opposite SPBs. MT depolymerization, possibly coupled to the sliding of MT plus ends past one another over a short distance, allows both nuclei to move in toward the site of cell fusion before karyogamy. These results reveal a novel mechanism for nuclear congression in which plus end-binding proteins and MT-based motors drive nuclear fusion via persistent attachment of depolymerizing plus ends. The consequences of plus end depolymerization-based nuclear congression are considered below.

Figure 10. **Model for nuclear congression in *S. cerevisiae*.** Nucleus is gray (black outline); SPB is a black circle; MTs are black lines; Kar3p-Bik1p plus end complex is a small gray circle. (A and B) MTs previously attached to the shmoo tip probe the cytoplasm to find oppositely oriented MTs. (C) The plus ends of MTs initiate interactions via Kar3p. (D) MT plus ends may slide past each other and cross-link, switching the MTs to a persistent depolymerization state. (E) SPBs move into the site of plus end interaction as MTs depolymerize, allowing nuclei to begin karyogamy.



Nuclear orientation is required for the fidelity of nuclear congression

Nuclear orientation to the shmoo tip depends on an intact actin cytoskeleton that is responsible for polarized growth (Hasek et al., 1987). Kar9p links the MT plus end to the actin network to guide the nucleus to the shmoo tip (Hwang et al., 2003). Loss of Kar9p results in severe nuclear orientation defects (Table S1; Miller and Rose, 1998). However, in these cells, nuclear congression did occur in the instances where interactions between MT plus ends were observed (Figs. 2 and 7). Conversely, for *kar3Δ* and *bik1Δ* cells, nuclear orientation did not confer success in congression (Fig. 2). These data suggest that Kar9p and the polarized actin network enhance the fidelity of nuclear congression by bringing MT tips into proximity upon cell wall breakdown, but they likely do not play a role in plus end interactions or MT shortening before karyogamy.

A consequence of nuclear orientation is the attachment of MTs to the shmoo tip (Maddox et al., 1999; Miller et al., 1999). In *kip2Δ* cells, attachment to the shmoo tip is reduced, but nuclear congression can occur (Figs. 2 and 3; Miller et al., 1998). Nuclear congression is reduced but successful in *kar9Δ* and *bik1Δ* cells that also have defective MT–shmoo tip attachments (Figs. 2 and 3). Therefore, like nuclear orientation, MT attachment to the shmoo tip is not required for karyogamy, but attachment may enhance the probability of contact between oppositely oriented MT plus ends in mating cells.

Nuclear congression

The sliding cross-bridge model predicts that Kar3p will cross-link and slide MTs past one another while depolymerizing MT minus ends (Rose, 1996). This model is supported by: (1) the failure of MT–MT interactions to occur in fixed *kar3-102* cells that were interpreted to be defective in lateral MT associations (Meluh and Rose, 1990); (2) the MT depolymerase activity of Kar3p that was initially reported to occur at the minus end in vitro (Endow et al., 1994); and (3) that Kar3p could cross-link

MTs along their length when associated with a second protein, Cik1p (Barrett et al., 2000). However, it has recently been shown that Kar3p is targeted to MT plus ends, and, in vitro, Kar3p-dependent MT depolymerization occurs at the plus ends (Maddox et al., 2003b; Sproul et al., 2005). In light of these facts, we reinvestigated nuclear congression and found that MT plus ends associate and shorten to promote nuclear fusion. Both Kar3p-GFP and Bik1p-3xGFP localize to MT plus ends that appear to interact at a single site in between both SPBs before nuclear congression (Fig. 5 and Fig. S1). Additionally, no detectable overlap zone is present when MTs are imaged during nuclear congression (Fig. 6). It should be noted that the spreading of the Bik1p-3xGFP signal during the later stages of nuclear congression could represent a small overlap zone where Kar3p-dependent sliding occurred (Fig. 5). Finally, when rigor-bound *kar3-1p* is distributed along the length of the MT, the concentration of plus ends between SPBs is disrupted (Fig. 9 C). Because MT dynamics are regulated at the plus end in both the shmoo tip (Maddox et al., 1999) and in mitotic cells (Maddox et al., 2000; Tanaka et al., 2005), we propose that MT plus end depolymerization provides the motive force to move both nuclei together.

What molecules are required for plus end interactions and MT depolymerization during nuclear congression? In the absence of Kar3p, MT plus ends did not interact to perform nuclear congression (Fig. 9 and Fig. S3). Therefore, Kar3p is required for the interaction of MT plus ends. In contrast, Bik1p is required to allow MTs to persistently interact during nuclear congression. In the absence of Bik1p, oppositely oriented MTs often do not contact each other as a result of their short length and rapid depolymerization (Fig. S2). We suggest that Bik1p stabilizes MTs to allow persistent cross-linking to occur or that Bik1p acts to directly maintain MT–MT interactions. In *kip2Δ* cells, there is no mating defect, although MT length is similar to *bik1Δ* cells (Fig. 2 and Table S2), suggesting that short MTs do not prevent nuclear congression. The low level of

Bik1p that localizes to the MT plus ends is likely sufficient to promote nuclear congression in *kip2Δ* cells (Fig. 8 A). These data suggest that Kar3p links oppositely oriented MTs, whereas Bik1p may stabilize plus ends and/or promote plus end interactions.

MTs shorten after plus end interactions are established, indicating that depolymerization is favored over dynamic instability. Depolymerization could be triggered by Kar3p or Kip3p, a second motor protein that has MT depolymerase activity (Miller et al., 1998). *kip3Δ* cells did not have a mating defect (Table S2; Miller et al., 1998), so the contribution of Kip3p to nuclear congression in wild-type cells is likely minimal. One hypothesis is that Kar3p favors MT plus end depolymerization when bound to oppositely oriented MTs. The inhibition of MT shortening after cross-linking in *kar3-1* cells could reflect the role of Kar3p as the critical depolymerase during nuclear congression (Fig. 9, B and C). Alternatively, cell cycle regulation or structural changes in the MT could promote depolymerization.

How do Kar3p and Bik1p maintain plus end interactions and depolymerize oppositely oriented MT arrays? MT plus ends orient and remain proximal to each other after cell wall breakdown (Fig. 10, A and B). We propose that Kar3p-dependent motor activity cross-links oppositely oriented MT plus ends, initiating nuclear congression (Fig. 10, C and D). After the initial MT–MT interactions are established, Kar3p could slide antiparallel MTs over a short distance. Once cross-linked, coordinated depolymerization begins and Kar3p, along with Bik1p, maintains the association of shortening MT plus ends as the nuclei move inward (Fig. 10 E). Kar3p and Bik1p could be part of a protein “sleeve,” similar to a proposal for kinetochore–MT interactions in higher eukaryotes (Hill, 1985) around MT plus ends. Kar3p in the sleeve complex could then induce shortening of the MTs. Alternatively, the minus end motor activity of Kar3p could cross-link and attempt to slide the MTs past each other, generating forces on the plus ends that induce depolymerization. The spreading of Bik1p-3xGFP during nuclear congression could be a result of the sliding of plus ends past one another, generating a slight overlap zone (Figs. 5 and 6). In this model, MT plus ends could interact directly at their tips or could have a small region of overlap.

Parallels to pronuclear migration

How does nuclear congression compare with metazoan fertilization? In higher eukaryotes, dynein-dependent pronuclear migration precedes karyogamy (Gonczy et al., 1999; Payne et al., 2003). In budding yeast, dynein has no role in nuclear congression (Table S2). The plus end interaction mechanism of budding yeast could dominate the process as a result of the limited number of MTs nucleated at the SPB that must be stabilized to facilitate nuclear congression. During metazoan pronuclear migration, the relatively large number of MTs may promote MT–nuclear envelope interactions that favor dynein function. Could plus ends have a major function in pronuclear migration? Or is the plus end complex of nuclear congression more similar to the cross-linking of interpolar MTs in the central spindle mitosis? Further analysis of nuclear congression in budding yeast should provide insight into MT plus end–based force generation in vivo.

Materials and methods

Media and strain construction

Media composition and genetic techniques are described elsewhere (Rose and Broach, 1990). Geneticin (Invitrogen) or hygromycin B (CellGro) were used at a concentration of 300 μg/ml. α-Factor (Sigma-Aldrich) resuspended in distilled water was used at a final concentration of 8 μg/ml. 5-Fluoroorotic acid (Toronto Research Chemicals) was used at a concentration of 1 g/L.

S. cerevisiae strains and plasmids used in this study are listed in Table 1. *kar3Δ* strains and the Bik1p-3xGFP plasmid were provided by D. Dawson (Tufts University, Boston, MA) and D. Pellman (Dana Farber Cancer Center, Boston, MA), respectively. Deletion of genes was performed using the pFA6::MX vectors (Wach et al., 1994; Longtine et al., 1998). GFP-Tub1p (Straight et al., 1997) and CFP-Tub1p (provided by M. Segal, University of Cambridge, Cambridge, UK) was linearized with *Stu*I before transformation, whereas Bik1p-3xGFP was linearized with *Nsi*I before integration (Carvalho et al., 2004).

Pheromone and mating assay growth conditions

Cells were grown to early to midexponential phase in YPD (yeast extract/peptone/glucose) or appropriate selective media at 32°C except for *kar3Δ* strains, which were grown at 25°C. All subsequent manipulations were performed at 32°C. For pheromone treatment, MATα cells were collected by centrifugation and resuspended in YPD supplemented with α-factor. Cells were incubated for 90–120 min, collected, and resuspended in distilled water before imaging.

For mating assays, MATα and MATα cells were grown to early to midexponential phase in YPD or the appropriate selective media. 500 μl of cells from each mating type were mixed, transferred into a 1-ml syringe, and collected on a 13-mm, 0.45-μm membrane (Millipore). The membrane was placed on a 60 × 15 mm YPD plate with the collected cells facing up for 60–120 min. Cells were resuspended by placing the filter paper into 500 μl of distilled water, vortexed to release the cells from the membrane, collected by centrifugation, and resuspended in distilled water before imaging. Cells were imaged on yeast complete media slabs supplemented with 25% gelatin. If cells were arrested with mating pheromone, the slabs were supplemented with 20 μg/ml α-factor.

Image acquisition and data analysis

All images were acquired using spinning disk confocal microscopy as previously described (Maddox et al., 2003a) except where noted. Wide-field images were acquired with a 100× NA 1.4 differential interference contrast objective on an upright microscope (Eclipse E-600; Nikon) or an inverted microscope (TE-2000; Nikon). Image acquisition was performed as previously described (Molk et al., 2004). The epifluorescence exposure time (2 × 2 binning) was 300–400 ms, whereas the differential interference contrast exposure time was 100–250 ms. Five-plane Z-series of 0.50-μm steps were acquired every 7–120 s and compiled into a single maximum projection image for each time point.

Imaging processing and fluorescence intensity measurements were performed in MetaMorph software (Universal Imaging Corp.) as previously described (Molk et al., 2004). γ adjustments for image presentation were performed in MetaMorph after data analysis was completed, and any brightness or contrast adjustments were performed in CorelDRAW10 (Corel Co.). Nuclear orientation to the shmoo tip was scored as wild-type if the GFP-Tub1p-marked SPB was either within or near the base of the mating projection. Aberrant nuclear orientation was recorded when the SPB was in the half of the cell body distal from the shmoo tip. The amount of time GFP-Tub1p fluorescence extended from the SPB to the shmoo tip during time-lapse imaging was recorded as the degree of persistence. Images were calibrated before analysis, and distances were recorded from projections of compiled 5-plane Z-series using either the single line tool or the calipers tool in MetaMorph to a linked Microsoft Excel spreadsheet. Nuclear congression was scored as defective if SPBs were visibly separated in the fluorescence image >0.5 μm after cell fusion occurred in still images. Successful nuclear congression in living cells was noted when both SPBs migrated toward each other and associated persistently. Rarely, time-lapse videos did not record SPB fusion and bud formation, possibly introducing a slight overestimate in the percentage of successful nuclear congression.

Online supplemental material

10 videos are included that display shmoo tip attachment (Video 1), Bik1p-3xGFP localization in the shmoo tip (Videos 2, 6, and 7), nuclear congression in wild-type cells (Videos 3 and 4), and MT behavior in karyogamy mutants (Videos 5, 8, 9, and 10). Additionally, three supplemental figures show Kar3p-GFP localization in wild-type cells (Fig. S1),

Table 1. *S. cerevisiae* strains and plasmids used in this study

Strain name	Relevant genotype	Source or reference
DC 49-7.1 C	MAT α <i>ura3-52 trp1-289 leu2-3, 112 arg4Δ57</i>	D. Dawson ^A
DC 48-5.1 C	MAT α <i>his3Δ1 ura3-52 trp1-289 arg4Δ42</i>	D. Dawson
TRS 108-5	MAT α <i>ura3-52 trp1-289 leu2-3, 112 arg4Δ57 kar3Δ::KAN^r pMR820</i>	D. Dawson
TRS 107-6	MAT α <i>his3Δ1 ura3-52 trp1-289 arg4Δ42 kar3Δ::KAN^r pMR820</i>	D. Dawson
YEF 473A	MAT α <i>trp1Δ63 leu2Δ1 ura3-52 his3Δ200 lys2-801</i>	Bi and Pringle, 1996
YEF 473B	MAT α <i>trp1Δ63 leu2Δ1 ura3-52 his3Δ200 lys2-801</i>	Bi and Pringle, 1996
GT1	MAT α <i>trp1Δ63 leu2Δ1 ura3-52 his3Δ200 lys2-801 GFP-TUB1::URA3</i>	Maddox et al., 2000
KBY 5026	MAT α <i>trp1Δ63 leu2Δ1 ura3-52 his3Δ200 lys2-801 kip3Δ::KAN^r GFP-TUB1::URA3</i>	J. Sims ^B
KBY 5049	MAT α <i>trp1Δ63 leu2Δ1 ura3-52 his3Δ200 lys2-801 kip2Δ::HB^r GFP-TUB1::URA3</i>	J. Sims
KBY 5058	MAT α <i>trp1Δ63 leu2Δ1 ura3-52 his3Δ200 lys2-801 kar9Δ::LEU2 GFP-TUB1::URA3</i>	J. Sims
KBY 9258	MAT α <i>trp1Δ63 leu2Δ1 ura3-52 his3Δ200 lys2-801 GFP-TUB1::URA3</i>	This study
KBY 9261	MAT α <i>trp1Δ63 leu2Δ1 ura3-52 his3Δ200 lys2-801 dhc1Δ::HIS3 GFP-TUB1::URA3</i>	This study
KBY 9262	MAT α <i>trp1Δ63 leu2Δ1 ura3-52 his3Δ200 lys2-801 dhc1Δ::HIS3 GFP-TUB1::URA3</i>	This study
KBY 9291	MAT α <i>trp1Δ63 leu2Δ1 ura3-52 his3Δ200 lys2-801 GFP-TUB1::URA3 kar9Δ::LEU2</i>	This study
KBY 9293	MAT α <i>trp1Δ63 leu2Δ1 ura3-52 his3Δ200 lys2-801 kar3Δ::TRP1</i>	This study
KBY 9313	MAT α <i>trp1Δ63 leu2Δ1 ura3-52 his3Δ200 lys2-801 kar3Δ::TRP1 GFP-TUB1::URA3</i>	This study
KBY 9306	MAT α <i>trp1Δ63 leu2Δ1 ura3-52 his3Δ200 lys2-801 GFP-TUB1::URA3 bik1Δ::TRP1</i>	This study
KBY 9308	MAT α <i>trp1Δ63 leu2Δ1 ura3-52 his3Δ200 lys2-801 GFP-TUB1::URA3 bik1Δ::TRP1</i>	This study
KBY 9311	MAT α <i>trp1Δ63 leu2Δ1 ura3-52 his3Δ200 lys2-801 GFP-TUB1::URA3 kip2Δ::KAN^r</i>	This study
KBY 9312	MAT α <i>trp1Δ63 leu2Δ1 ura3-52 his3Δ200 lys2-801 GFP-TUB1::URA3 kip3Δ::KAN^r</i>	This study
KBY 9316	MAT α <i>trp1Δ63 leu2Δ1 ura3-52 his3Δ200 lys2-801 bik1Δ::TRP1</i>	This study
KBY 9317	MAT α <i>trp1Δ63 leu2Δ1 ura3-52 his3Δ200 lys2-801 bik1Δ::TRP1</i>	This study
KBY 9318	MAT α <i>trp1Δ63 leu2Δ1 ura3-52 his3Δ200 lys2-801 BIK1::3xGFP-TRP1</i>	This study
KBY 9319	MAT α <i>ura3-52 trp1-289 leu2-3, 112 arg4Δ57 kar3Δ::KAN^r BIK1::3xGFP-TRP1 pMR820</i>	This study
KBY 9320	MAT α <i>his3Δ1 ura3-52 trp1-289 arg4Δ42 kar3Δ::KAN^r BIK1::3xGFP-TRP1 pMR820</i>	This study
KBY 9322	MAT α <i>ura3-52 trp1-289 leu2-3, 112 arg4Δ57 kar3Δ::KAN^r BIK1::3xGFP-TRP1</i>	This study
KBY 9323	MAT α <i>his3Δ1 ura3-52 trp1-289 arg4Δ42 kar3Δ::KAN^r BIK1::3xGFP-TRP1</i>	This study
KBY 9324	MAT α <i>trp1Δ63 leu2Δ1 ura3-52 his3Δ200 lys2-801 kip2Δ::KAN^r BIK1::3xGFP-TRP1</i>	This study
KBY 9325	MAT α <i>trp1Δ63 leu2Δ1 ura3-52 his3Δ200 lys2-801 BIK1::3xGFP-TRP1 CFP-TUB1::URA3</i>	This study
KBY 9337	MAT α <i>trp1Δ63 leu2Δ1 ura3-52 his3Δ200 lys2-801 BIK1::3xGFP-TRP1</i>	This study
Plasmid name	Relevant genotype	Source or reference
pMR820	KAR3-URA3 (Amp ^r)	Meluh and Rose, 1990
pAFS125	GFP-TUB1-URA3 (Amp ^r)	Straight et al., 1997
CFP-Tub1p	CFP-TUB1-URA3 (Amp ^r)	M. Segal ^C
Bik1p-3xGFP	BIK1-3xGFP-TRP1 (Amp ^r)	Carvalho et al., 2004

^ATufts University, Boston, MA.^BUniversity of North Carolina, Chapel Hill, NC.^CUniversity of Cambridge, Cambridge, UK.

MT behavior in *bik1 Δ* cells (Fig. S2), and Bik1p-3xGFP localization in *kar3 Δ* cells after cell fusion (Fig. S3). Table S1 shows measurements of nuclear orientation and cytoplasmic MT attachment to the shmoo tip. Table S2 shows nuclear congression efficiency among karyogamy mutants. Online supplemental material is available at <http://www.jcb.org/cgi/content/full/jcb.200510032/DC1>.

We thank David Bouck, Bob Goldstein, Paul Maddox, Chad Pearson, Mark Rose, Jennifer Sims, and members of the Bloom and Salmon laboratories for assistance with microscopy, strains, reagents, critical readings of the manuscript, and advice. We are especially grateful to David Pellman for providing the Bik1p-3xGFP plasmid and Dean Dawson for supplying *kar3 Δ* strains.

This work was funded by the Human Frontier Science Program grant RGP29/2003 (to E.D. Salmon) and the National Institutes of Health grants GM-24364 (to E.D. Salmon), GM-60678 (to E.D. Salmon), and GM-32238 (to K. Bloom).

Submitted: 5 October 2005

Accepted: 29 November 2005

References

Barrett, J.G., B.D. Manning, and M. Snyder. 2000. The Kar3p kinesin-related protein forms a novel heterodimeric structure with its associated protein

Cik1p. *Mol. Biol. Cell.* 11:2373–2385.

Berlin, V., C.A. Styles, and G.R. Fink. 1990. BIK1, a protein required for microtubule function during mating and mitosis in *Saccharomyces cerevisiae*, colocalizes with tubulin. *J. Cell Biol.* 111:2573–2586.

Bi, E., and J.R. Pringle. 1996. ZDS1 and ZDS2, genes whose products may regulate Cdc42p in *Saccharomyces cerevisiae*. *Mol. Cell. Biol.* 16:5264–5275.

Carvalho, P., M.L. Gupta Jr., M.A. Hoyt, and D. Pellman. 2004. Cell cycle control of kinesin-mediated transport of Bik1 (CLIP-170) regulates microtubule stability and dynein activation. *Dev. Cell.* 6:815–829.

Endow, S.A., S.J. Kang, L.L. Satterwhite, M.D. Rose, V.P. Skeen, and E.D. Salmon. 1994. Yeast Kar3 is a minus-end microtubule motor protein that destabilizes microtubules preferentially at the minus ends. *EMBO J.* 13:2708–2713.

Gonczy, P., S. Pichler, M. Kirkham, and A.A. Hyman. 1999. Cytoplasmic dynein is required for distinct aspects of MTOC positioning, including centrosome separation, in the one cell stage *Caenorhabditis elegans* embryo. *J. Cell Biol.* 147:135–150.

Hasek, J., I. Rupes, J. Svobodova, and E. Streiblova. 1987. Tubulin and actin topology during zygote formation of *Saccharomyces cerevisiae*. *J. Gen. Microbiol.* 133:3355–3363.

Hill, T.L. 1985. Theoretical problems related to the attachment of microtubules to kinetochores. *Proc. Natl. Acad. Sci. USA.* 82:4404–4408.

Hwang, E., J. Kusch, Y. Barral, and T.C. Huffaker. 2003. Spindle orientation in *Saccharomyces cerevisiae* depends on the transport of microtubule ends along polarized actin cables. *J. Cell Biol.* 161:483–488.

- Kurihara, L.J., C.T. Beh, M. Latterich, R. Schekman, and M.D. Rose. 1994. Nuclear congression and membrane fusion: two distinct events in the yeast karyogamy pathway. *J. Cell Biol.* 126:911–923.
- Lee, W.L., J.R. Oberle, and J.A. Cooper. 2003. The role of the lissencephaly protein Pac1 during nuclear migration in budding yeast. *J. Cell Biol.* 160:355–364.
- Lin, H., P. de Carvalho, D. Kho, C.Y. Tai, P. Pierre, G.R. Fink, and D. Pellman. 2001. Polyploids require Bik1 for kinetochore-microtubule attachment. *J. Cell Biol.* 155:1173–1184.
- Longtine, M.S., A. McKenzie III, D.J. Demarini, N.G. Shah, A. Wach, A. Brachat, P. Philippsen, and J.R. Pringle. 1998. Additional modules for versatile and economical PCR-based gene deletion and modification in *Saccharomyces cerevisiae*. *Yeast.* 14:953–961.
- Maddox, P., E. Chin, A. Mallavarapu, E. Yeh, E.D. Salmon, and K. Bloom. 1999. Microtubule dynamics from mating through the first zygotic division in the budding yeast *Saccharomyces cerevisiae*. *J. Cell Biol.* 144:977–987.
- Maddox, P.S., K.S. Bloom, and E.D. Salmon. 2000. The polarity and dynamics of microtubule assembly in the budding yeast *Saccharomyces cerevisiae*. *Nat. Cell Biol.* 2:36–41.
- Maddox, P.S., B. Moree, J.C. Canman, and E.D. Salmon. 2003a. Spinning disk confocal microscope system for rapid high-resolution, multimode, fluorescence speckle microscopy and green fluorescent protein imaging in living cells. *Methods Enzymol.* 360:597–617.
- Maddox, P.S., J.K. Stemple, L. Satterwhite, E.D. Salmon, and K. Bloom. 2003b. The minus end-directed motor Kar3 is required for coupling dynamic microtubule plus ends to the cortical shmoo tip in budding yeast. *Curr. Biol.* 13:1423–1428.
- Maekawa, H., T. Usui, M. Knop, and E. Schiebel. 2003. Yeast Cdk1 translocates to the plus end of cytoplasmic microtubules to regulate bud cortex interactions. *EMBO J.* 22:438–449.
- Meluh, P.B., and M.D. Rose. 1990. KAR3, a kinesin-related gene required for yeast nuclear fusion. *Cell.* 60:1029–1041.
- Miller, R.K., and M.D. Rose. 1998. Kar9p is a novel cortical protein required for cytoplasmic microtubule orientation in yeast. *J. Cell Biol.* 140:377–390.
- Miller, R.K., K.K. Heller, L. Frisen, D.L. Wallack, D. Loayza, A.E. Gammie, and M.D. Rose. 1998. The kinesin-related proteins, Kip2p and Kip3p, function differently in nuclear migration in yeast. *Mol. Biol. Cell.* 9:2051–2068.
- Miller, R.K., D. Matheos, and M.D. Rose. 1999. The cortical localization of the microtubule orientation protein, Kar9p, is dependent upon actin and proteins required for polarization. *J. Cell Biol.* 144:963–975.
- Molk, J.N., S.C. Schuyler, J.Y. Liu, J.G. Evans, E.D. Salmon, D. Pellman, and K. Bloom. 2004. The differential roles of budding yeast Tem1p, Cdc15p, and Bub2p protein dynamics in mitotic exit. *Mol. Biol. Cell.* 15:1519–1532.
- O'Toole, E.T., M. Winey, and J.R. McIntosh. 1999. High-voltage electron tomography of spindle pole bodies and early mitotic spindles in the yeast *Saccharomyces cerevisiae*. *Mol. Biol. Cell.* 10:2017–2031.
- Payne, C., V. Rawe, J. Ramalho-Santos, C. Simerly, and G. Schatten. 2003. Preferentially localized dynein and perinuclear dynactin associate with nuclear pore complex proteins to mediate genomic union during mammalian fertilization. *J. Cell Sci.* 116:4727–4738.
- Pellman, D., M. Bagget, Y.H. Tu, G.R. Fink, and H. Tu. 1995. Two microtubule-associated proteins required for anaphase spindle movement in *Saccharomyces cerevisiae*. *J. Cell Biol.* 130:1373–1385.
- Polaina, J., and J. Conde. 1982. Genes involved in the control of nuclear fusion during the sexual cycle of *Saccharomyces cerevisiae*. *Mol. Gen. Genet.* 186:253–258.
- Rose, A.B., and J.R. Broach. 1990. Propagation and expression of cloned genes in yeast: 2-microns circle-based vectors. *Methods Enzymol.* 185:234–279.
- Rose, M.D. 1996. Nuclear fusion in the yeast *Saccharomyces cerevisiae*. *Annu. Rev. Cell Dev. Biol.* 12:663–695.
- Sheeman, B., P. Carvalho, I. Sagot, J. Geiser, D. Kho, M.A. Hoyt, and D. Pellman. 2003. Determinants of *S. cerevisiae* dynein localization and activation: implications for the mechanism of spindle positioning. *Curr. Biol.* 13:364–372.
- Sproul, L.R., D.J. Anderson, A.T. Mackey, W.S. Saunders, and S.P. Gilbert. 2005. Cik1 targets the minus-end kinesin depolymerase kar3 to microtubule plus ends. *Curr. Biol.* 15:1420–1427.
- Straight, A.F., W.F. Marshall, J.W. Sedat, and A.W. Murray. 1997. Mitosis in living budding yeast: anaphase A but no metaphase plate. *Science.* 277:574–578.
- Tanaka, K., N. Mukae, H. Dewar, M. van Breugel, E.K. James, A.R. Prescott, C. Antony, and T.U. Tanaka. 2005. Molecular mechanisms of kinetochore capture by spindle microtubules. *Nature.* 434:987–994.
- Tirnauer, J.S., E. O'Toole, L. Berrueta, B.E. Bierer, and D. Pellman. 1999. Yeast Bim1p promotes the G1-specific dynamics of microtubules. *J. Cell Biol.* 145:993–1007.
- Wach, A., A. Brachat, R. Pohlmann, and P. Philippsen. 1994. New heterologous modules for classical or PCR-based gene disruptions in *Saccharomyces cerevisiae*. *Yeast.* 10:1793–1808.